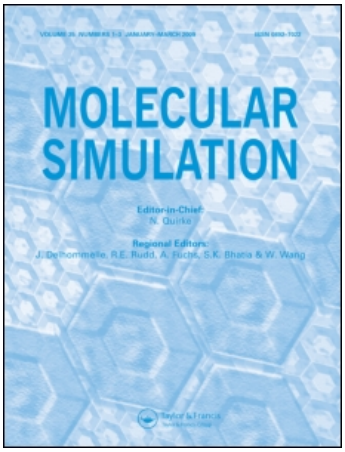

Molecular Simulation
Publication details, including instructions for authors and subscription information:
http://www.informaworld.com/smpp/title~content=t713644482

A novel method to predict the glass transition of 70% glycerol aqueous solution

Bochun Wang[a]; Dai-Xi Li[a]; Bao-Lin Liu[a]; Cheng-Lung Chen[b]
[a] School of Medical Instruments and Food Science, University of Shanghai for Science and Technology, Shanghai, P. R. China [b] Department of Chemistry, National Sun Yat-Sen University, Kaohsiung, Taiwan, R.O.C

Online publication date: 24 November 2010

To cite this Article Wang, Bochun , Li, Dai-Xi , Liu, Bao-Lin and Chen, Cheng-Lung(2010) 'A novel method to predict the glass transition of 70% glycerol aqueous solution', Molecular Simulation, 36: 13, 1025 — 1030
To link to this Article: DOI: 10.1080/08927022.2010.499148
URL: http://dx.doi.org/10.1080/08927022.2010.499148

Molecular Simulation
Vol. 36, No. 13, November 2010, 1025–1030

Taylor & Francis
Taylor & Francis Group

A novel method to predict the glass transition of 70% glycerol aqueous solution

Bochun Wang[a], Dai-Xi Li[a]*, Bao-Lin Liu[a] and Cheng-Lung Chen[b]

[a]*School of Medical Instruments and Food Science, University of Shanghai for Science and Technology, 516, Jungong Rd, Shanghai 200093, P. R. China;* [b]*Department of Chemistry, National Sun Yat-Sen University, Kaohsiung 80424, Taiwan, R.O.C*

(*Received 7 January 2010; final version received 3 June 2010*)

Vitrification has been used to successfully cryopreserve cells and tissues for over 60 years. Glass transition temperature (T_g) of the vitrification is a critical parameter, which has been investigated experimentally. In this study, an isothermal–isobaric molecular simulation (NPT-MD) is proposed to investigate the glass transition and T_g of such vitrification solution. The cohesive energy density, solubility parameter (δ) and bulk modulus of the solution during the process of the glass transition are investigated as well. The results indicate that these properties as functions of temperature can give a definite inflexion; thus, these properties can be used to predict T_g more accurately than the heat capacity (C_p), density (ρ), volume (V) and radial distribution function (rdf). At the same time, the predicted values of T_g agree well with the experimental results. Therefore, molecular dynamics simulation is a potential method for investigating the glass transition and T_g of the vitrification solutions.

Keywords: molecular dynamics simulation; glass transition temperature; vitrification; cryoprotectant

1. Introduction

Cryopreservation of vital organs is critical in the treatment of patients with organ failure [1,2]. Vitrification has been proposed to be the best way for the cryopreservation of tissues and organs [3–5]. As one of the critical parameters for cryopreservation by vitrification, the glass transition temperature (T_g) has been investigated primarily by experimental approaches, such as the differential scanning calorimeter (DSC) and the dynamic mechanical analyser (DMA) [6].

Although T_g can be measured experimentally, the structural change in vitrification solution at different temperatures is difficult to be investigated and analysed [7–13]. On the other hand, computer simulation can provide very useful structural information and help experimentalists to verify their result. Therefore, predicting T_g of a vitrification solution by simulation may be a novel and effective method [14].

Because glycerol can prevent aqueous solution from forming ice crystals, glycerol, as an important cryoprotectant, has been used for successful cryopreservation of many types of cells and tissues [15–34] since 1969, such as semen [21,32], oocytes [23] and pig and human liver slices [29], testicular tissue [30], black chokeberry [31] and so on. Generally, ice crystals can damage cells or organs to be cryopreserved. At the same time, glycerol can also make aqueous solution vitrify at very low temperature.

Although many studies have been performed in order to understand the cryopreservation mechanism of glycerol, it is still far from a complete understanding of its biological functions. The molecular mechanisms of the glass transition of solutions are worthy to be defined.

In this paper, the cohesive energy density (CED), the solubility parameter (δ) and the bulk modulus of the glycerol aqueous solution are investigated by molecular dynamics (MD) simulation [35–38]. These properties can be used to evaluate intermolecular interaction [39] which cannot be determined by measurements. Based on the simulation results, the mechanism of glass transition is investigated.

2. Theory and method

2.1 Theory

Most thermodynamic properties, such as heat capacity, volume and density, are functions of temperature. In a uniphase, these properties change gradually with temperature. But when a substance transforms from one phase to another, the linear relationship between some thermodynamic properties and temperature (e.g. the relationship between kinetic energy and temperature) might continue without any change. Other thermodynamic properties showed a discontinuity at a specific temperature in the plot of state parameter vs. temperature during the process of the phase transition. Thus, the phase transition temperature can be predicted by tracking such discontinuity. Similarly, for the vitrification solution, those thermodynamic properties, which have an obvious inflection point or jump interval during the glass transition,

*Corresponding author. Email: blliuk@163.com

ISSN 0892-7022 print/ISSN 1029-0435 online

DOI: 10.1080/08927022.2010.499148
http://www.informaworld.com

can be used to predict the glass transition temperature. In order to validate the above prediction, in this paper, the glass transition temperature of the glycerol aqueous solution (70%, wt%) was investigated using the MD simulation.

The first groups of properties to be investigated here are the CED and the solubility parameter (δ) [40]. In molecular simulations, the CED corresponds to the cohesive energy per unit volume. The cohesive energy is defined as the amount of energy per mole of a material if all intermolecular forces are eliminated. In other words, the cohesive energy of the solid or liquid is the energy required to break the molecules into isolated molecules.

According to the above definition, the CED includes all intermolecular interactions per unit volume, such as electrostatic interaction and van der Waals interaction. Both CED and its square root (the solubility parameter, δ) are important parameters because they can not only be used to determine the intersolubility between different compositions, but also indicate the strength of the interaction between molecules. By analysing these parameters, the structure of the vitrification solutions at the glass transition temperature can be investigated.

Another property to be investigated is the bulk modulus. The bulk modulus elasticity is a property characterising the compressibility, i.e. how the volume per unit of fluid can be changed when changing the pressure working upon it. The bulk modulus elasticity can be expressed as

$$E = -\mathrm{d}p/(\mathrm{d}V/V), \tag{1}$$

or

$$E = \mathrm{d}p/(\mathrm{d}\rho/\rho), \tag{2}$$

where E is the bulk modulus elasticity; $\mathrm{d}p$, $\mathrm{d}V$ and $\mathrm{d}\rho$ are the differential change in pressure, volume and density, respectively; V and ρ are the initial volume and density, respectively. Any increase in the pressure will decrease the volume. Meanwhile, any decrease in the volume will increase the density. A large bulk modulus indicates a relatively incompressible fluid [41].

2.2 Method

The modules of Minimiser, Discover and Amorphous Cell Tools in the commercial software package of Materials Studio (Accelrys, San Diego, CA, USA) are used to perform the isothermal–isobaric molecular dynamic simulations (NPT-MD) with the polymer consistent force field (PCFF) [42]. The cut-off distances for both van der Waals and electrostatic interaction are 9.50 Å. Also, the long-range correction [43] is applied. In the PCFF, van der Waals energy is described by the Lennard-Jones (9-6) potential [44]. The electrostatic energy is calculated using the Ewald summation method [45] since it calculates long-range interactions more accurately.

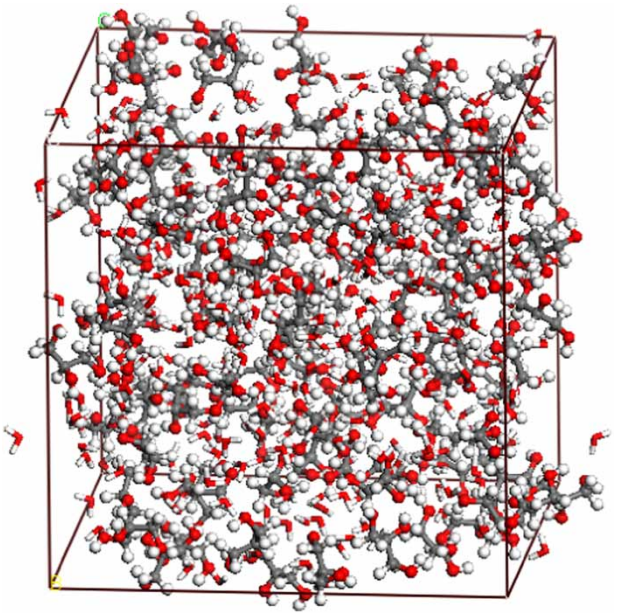

Figure 1. Amorphous cell for 70% glycerol aqueous solution. (The amorphous cell of 70% (wt%) glycerol aqueous solution is composed of 114 glycerol molecules with 250 water molecules. For clarity, glycerol molecules are represented by ball and stick, and water molecules are represented by stick.)

For the simulation of 70% (wt%) glycerol aqueous solution, temperature and pressure (1 atm) are controlled by the Andersen method [46]. The amorphous cell is composed of 114 glycerol molecules with 250 water molecules (Figure 1). The potential energy of the system is first minimised using the Smart Minimiser method. The molecular simulation is performed from 90 to 250 K with an interval of 20 K, and time step as 1 fs. The time used for equilibrium of the glycerol aqueous solution at each temperature is 10 ns. After the equilibrium is reached, the production simulation is continued to perform several times in order to obtain an average. For each production simulation at each temperature, the simulation time is 3 ns. Each trajectory is sampled every 250 fs. As a result, a total of 12,000 structures are generated for the analysis.

3. Results and discussion

3.1 The alternation of CED and solubility parameter during glass transition

The cohesion state and physical properties of substances are determined by the spatial arrangement of their molecules. The interactions between molecules relate directly to the special arrangement of the molecules.

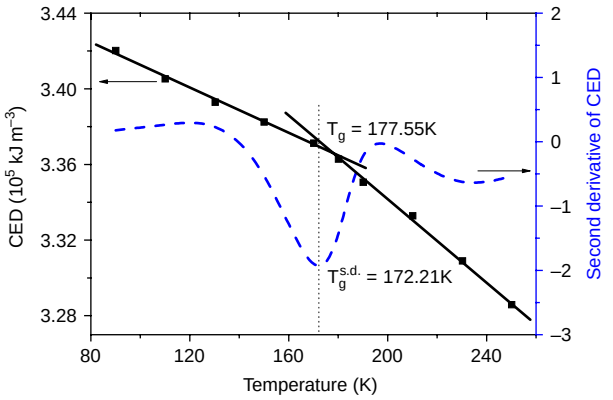

Figure 2. Curves of CED vs. temperature for 70% glycerol aqueous solution. (Curve of CED indicates that the lower the temperature, the higher the CED. But the increase in the CED during the decrease in temperature is discontinuous, and the inflexion point T_g is predicted at 172.21–177.55 K.)

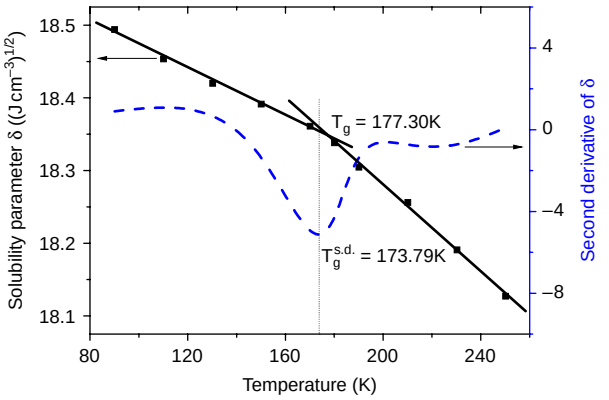

Figure 3. Curves of solubility parameter vs. temperature for 70% glycerol aqueous solution. (The curve of the solubility parameter also has the same regularity as that of the CED; the predicted T_g is 173.79–177.30 K. Solubility parameter agrees well with CED.)

So, the strength of intermolecular interactions can be characterised by the CED. Therefore, both the CED and its square root (the so-called solubility parameter, δ) are key thermodynamic parameters of solutions.

Therefore, the change in the CED and δ with temperature should reveal the relationship between the structure and properties of the solution. The calculated value of the CED of the solution as a function of temperatures is shown in Figure 2.

It can be seen from Figure 2 that CED increases linearly with the decrease in temperature at supercooled liquid or glass state, respectively. In order to predict accurately the inflexion point of the curve, the second derivative was used, which gave a minimum value at 172.21 K. According to the inflexion, the data of CED were divided into two groups. When the two groups of data were linearly fitted and extrapolated, they intercrossed at 177.55 K.

The curve of the solubility parameter (δ) as a function of temperature (Figure 3) is similar to that of the CED. Our calculated results of the CED and δ with temperature shows the same pattern as Stefanis' report [47]. Though these values differ from those of the Stephanis report about pure water, the same pattern suggests that our results are reliable. When the curve of the solubility parameter (δ) as a function of temperature (Figure 3) was analysed by the same method, the inflexion was given at 173.79–177.30 K.

As a main intermolecular interaction, the electrostatic interaction also contributes to solubility parameter, namely, the solubility parameter derived from the electrostatic interaction (δ_{es}). It is very interesting that the curve of δ_{es} yields a more obvious inflexion than that of the total solubility parameter (δ) does (Figure 4). A peak of its curve gives a definitely glass transition value of 171.75–173.00 K according to the above analysis methods.

3.2 The alternation of the bulk modulus during glass transition

The bulk modulus gives alterations in volume of a solid or liquid substance as the pressure is changed. From the statistical analysis result of the elastic properties originated from the molecular simulation of the glycerol aqueous solution, the bulk modulus curves under different temperatures are shown in Figure 5. At the same time, the bulk modulus of the solution at 300 K was calculated in order to validate the reliability of the molecular simulation. The value of the bulk modulus of the solution at 300 K yields 4.37 GPa, which agrees well with Loubeyre's reported value of 4.26 GPa [48].

Generally, solution is easier to be compressed than glass, the pattern of which agrees with our simulation.

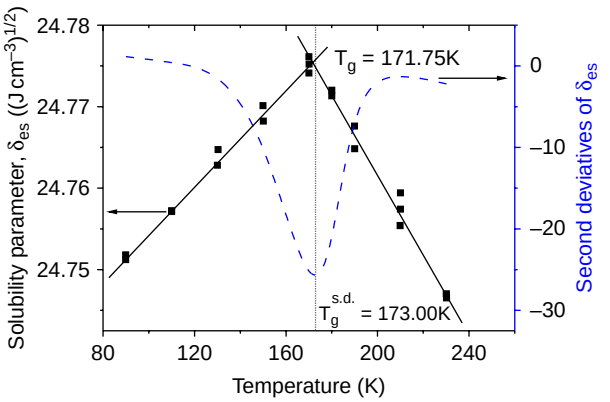

Figure 4. Curves of solubility parameter derived from electrostatic interaction vs. temperature.

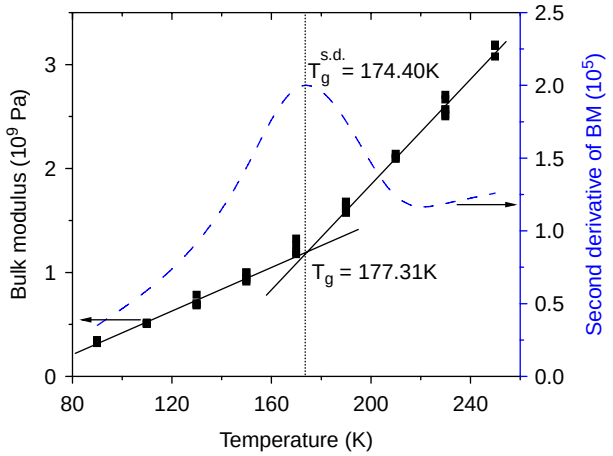

Figure 5. Curves of bulk modulus (BM) vs. temperature.

Moreover, judging from the bulk modulus curves under different temperatures, the inflexion temperature is the so-called glass transition temperature, 177.31–174.40 K.

3.3 Verification and comparison between predicted and experimental values of T_g

In order to verify the above predicted T_g values, here, the predicted values calculated from other methods as well as their corresponding experimental values were compared.

Since the practicability and reliability of the method to predict T_g in reference [42] have been proved by many reports [10,42,49], here, the heat capacity (C_p), density (ρ), cell volume (V) and the radial distribution function (rdf) at each temperature have also been calculated and analysed in order to predict the T_g of the glycerol aqueous solution (Figure 6). The predicted T_g values from these different physical properties of the glycerol aqueous solution are listed in Table 1. The second derivative of the property-temperature curve was also used to obtain accurate inflexion point of the curves in Figure 6 because the inflexion points in their property-temperature curves are amphibolous.

From the data in Table 1, it can be seen that both groups of the predicted T_g values agree well with the experimental values in the literature [15,17]. However, the

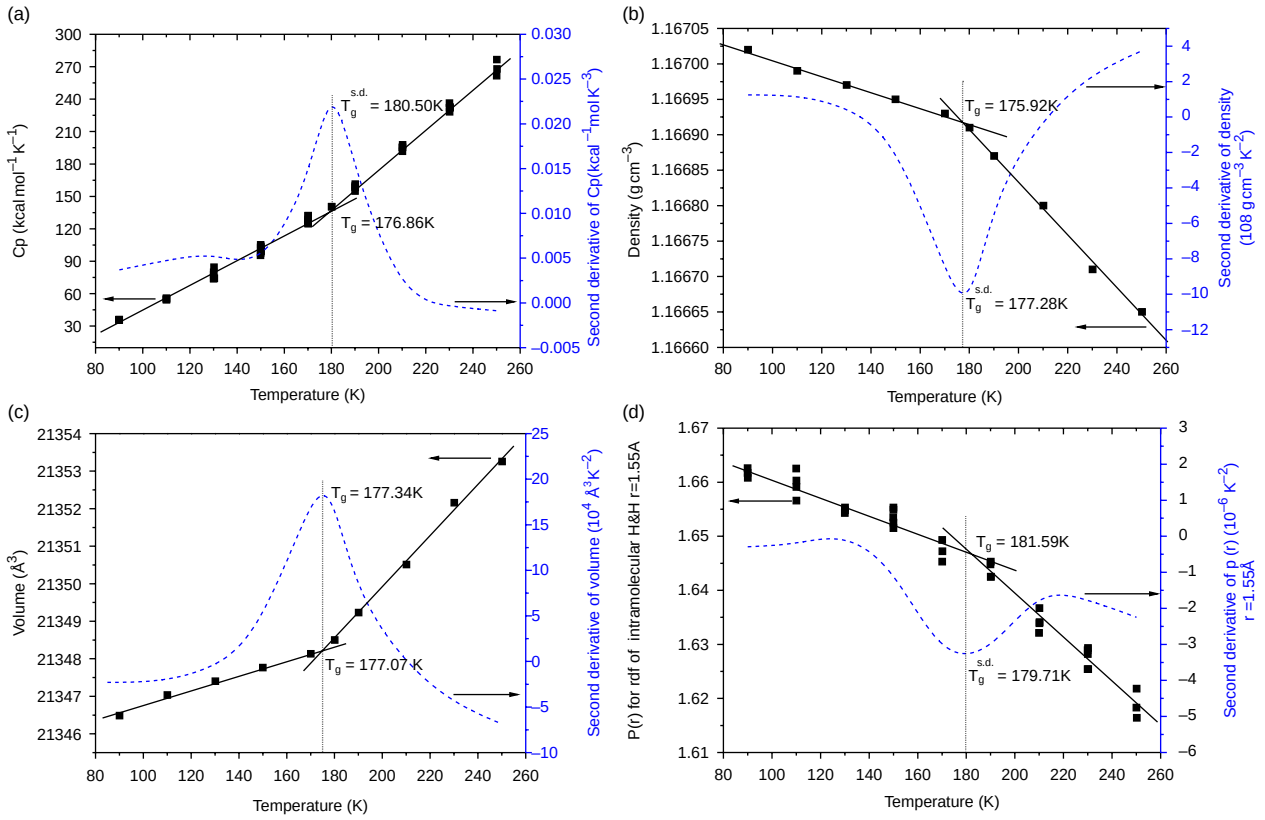

Figure 6. Curves of C_p, density, volume and rdf vs. temperature. (a), C_p curve; (b), density curve; (c), volume curve; (d), rdf curve from H to H with r = 1.55 Å. For clarity, the second derivative was used to accurately predict the inflexions of curves. The results indicate that the glass transition temperature is about 175.92–181.59 K, whose values are very near to the experimental values 168.11–173.94 K. The notation $T_g^{s.d.}$ denotes the glass transition temperature predicted by the second derivative; and T_g denotes the glass transition temperature predicted by linear fitting and extrapolation in this paper.)

Table 1. Comparison between the predicted and experimental T_g values of the glycerol aqueous solution.

New method	CED	Solubility parameter	δ_{es}	Bulk modulus
Predicted T_g (k)	172.21–177.55	173.79–177.30	171.75–173.00	174.40–177.31
Old method	Heat capacity	Density	Volume	rdf
Predicted T_g (k)	176.86–180.50	175.92–177.28	177.07–177.34	179.71–181.59
Experimental		168.11–173.94 [15,17,50]		

former predicted T_g values closer to the experimental values than the latter. These results prove that the new prediction method is also reasonable.

In addition, though all the above predicted values are slightly larger than the experimental ones, it is perhaps because the MD methods could not simulate a cooling rate as slow as the experimental one. Above all, the novel predicted method does work for researching the glass transition, especially, for predicting the glass transition temperature.

4. Summary and conclusions

Glass transition temperature (T_g) of the vitrification as a critical experimental parameter is investigated here using NPT-MD. The predicted results of the T_g values using the CED, solubility parameter (δ) and bulk modulus prove that these properties as functions of temperature can give more accurate prediction than typical physical properties (e.g. C_p, ρ, $V$and rdf) do. Therefore, MD simulation should be a useful method to investigate the glass transition and T_g of the vitrification solutions, and this simulation can help us to fully understand the mechanism of glass transition.

Acknowledgements

This research was supported by the National Science Foundation of China (50776060), NCET-07-0559, ESP at SIHL and Sh-LAD (S30503) and the Shanghai Development Funds (05EZ21).

References

[1] X. Wang, H. Chen, H. Yin, S.S. Kim, S. Lin Tan, and R.G. Gosden, *Fertility after intact ovary transplantation*, Nature 415 (2002), p. 385.

[2] B.L. Liu and J.J. McGrath, *Effects of two-step freezing on the ultrastructural components of murine osteoblast cultures*, Cryoletters 27 (2006), pp. 369–374.

[3] G.M. Fahy, D.R. Macfarlane, C.A. Angell, and H.T. Meryman, *Vitrification as an approach to cryopreservation*, Cryobiology 21 (1984), pp. 407–426.

[4] I.A. de Graaf, A.L. Draaisma, O. Schoeman, G.M. Fahy, G.M. Groothuis, and H.J. Koster, *Cryopreservation of rat precision-cut liver and kidney slices by rapid freezing and vitrification*, Cryobiology 54 (2007), pp. 1–12.

[5] W.F. Rall and G.M. Fahy, *Ice-free cryopreservation of mouse embryos at −196-degrees-C by vitrification*, Nature 313 (1985), pp. 573–575.

[6] F. Fraga, T. Salgado, J.A.R. Anon, and L.N. Regueira, *Determination of physical and structural parameters by DMA and DSC – Application to an epoxidic formulation*, J. Therm. Anal. 41 (1994), pp. 1543–1550.

[7] B.S. Kheirabadi and G.M. Fahy, *Permanent life support by kidneys perfused with a vitrifiable (7.5 molar) cryoprotectant solution*, Transplantation 70 (2000), pp. 51–57.

[8] Y. Hu, Y. Zhang, B.Y. Li, and Y. Ozaki, *Application of sample–sample two-dimensional correlation spectroscopy to determine the glass transition temperature of poly(ethylene terephthalate) thin films*, Appl. Spectrosc. 61 (2007), pp. 60–67.

[9] I. Weuts, D. Kempen, K. Six, J. Peeters, G. Verreck, M. Brewster, and G. Van den Mooter, *Evaluation of different calorimetric methods to determine the glass transition temperature and molecular mobility below T_g for amorphous drugs*, Int. J. Pharm. 259 (2003), pp. 17–25.

[10] Y. Tamai, *A practical method to determine glass transition temperature in MD simulation of mixed ionic glasses*, Chem. Phys. Lett. 351 (2002), pp. 99–104.

[11] S.N. Ganeriwala and H.A. Hartung, *Fourier-transform mechanical analysis (Ftma) to determine dynamic mechanical properties and glass-transition temperature of polymers*, Abstr. Pap. Am. Chem. Soc. 197 124-PMSE (1989).

[12] A. Baudot, B. Courbiere, V. Odagescu, B. Salle, C. Mazoyer, J. Massardier, and J. Lornage, *Towards whole sheep ovary cryopreservation*, Cryobiology 55 (2007), pp. 236–248.

[13] V. Berejnov, N.S. Husseini, O.A. Alsaied, and R.E. Thorne, *Effects of cryoprotectant concentration and cooling rate on vitrification of aqueous solutions*, J. Appl. Crystallogr. 39 (2006), pp. 244–251.

[14] I.I. Katkov and F. Levine, *Prediction of the glass transition temperature of water solutions: Comparison of different models*, Cryobiology 49 (2004), pp. 62–82.

[15] B. Wowk, M. Darwin, S.B. Harris, S.R. Russell, and C.M. Rasch, *Effects of solute methoxylation on glass-forming ability and stability of vitrification solutions*, Cryobiology 39 (1999), pp. 215–227.

[16] J.B. Derrick, M. Lind, and A.W. Rowe, *Metabolic integrity of human red cells subjected to a low glycerol-rapid freeze cryopreservation procedure*, Cryobiology 6 (1969), p. 260.

[17] J.B. Derrick, M. Lind, and A.W. Rowe, *Studies of metabolic integrity of human red blood cells after cryopreservation. I. Effects of low-glycerol-rapid-freeze preservation on energy status and intracellular sodium and potassium*, Transfusion 9 (1969), p. 317.

[18] J.B. Derrick, R. Mcconn, M.L. Sorovacu, and A.W. Rowe, *Studies of metabolic integrity of human red blood-cells after cryopreservation. 2. Effects of low-glycerol-rapid-freeze preservation on glycolysis*, Transfusion 12 (1972), pp. 400–404.

[19] G. Dayian and A.W. Rowe, *Cryopreservation of human platelets for transfusion – Glycerol-glucose, moderate rate cooling procedure*, Cryobiology 13 (1976), pp. 1–8.

[20] J. Frim and P. Mazur, *Cryopreservation of human-granulocytes using glycerol*, Cryobiology 16 (1979), pp. 598–598.

[21] H.J. Vonglander and U. Colditz, *Comparison between cryoprotective potentials of glycerol, dimethylsulfoxide, dimethylformamide, and ethylene-glycol in cryopreservation of human-semen*, Zentralblatt Für Gynäkologie 103 (1981), pp. 840–848.

[22] H.E. Bernard, B.J. Fuller, and I. Craft, *Recovery of 2-cell mouse embryos after cryopreservation using low glycerol concentrations and normothermic cryoprotectant equilibration*, Cryoletters 3 (1982), pp. 326–326.

[23] A. Bernard and B. Fuller, *The effect of glycerol on cryopreservation of mouse oocytes*, Cryobiology 20 (1983), pp. 717–717.
[24] M.J. Taylor and T.J. Duffy, *Cryopreservation of isolated pancreatic-islets – The pattern of insulin-secretion after slow cooling and warming in the presence of either dimethylsulfoxide or glycerol*, Transplant. Proc. 15 (1983), pp. 2196–2196.
[25] S.M. Mutetwa and E.R. James, *Cryopreservation of plasmodium-chabaudi. 1. Protection by glycerol and dimethylsulfoxide during cooling and by glucose following thawing*, Cryobiology 21 (1984), pp. 329–339.
[26] P.S. Fiser and R.W. Fairfull, *Interaction of glycerol level, cooling velocity, and the osmolality of skim-milk diluents used for cryopreservation of ram spermatozoa*, Cryobiology 21 (1984), pp. 711–712.
[27] T. Takeda, *Cryopreservation of mouse morulae in propylene-glycol or glycerol*, Theriogenology 27 (1987), pp. 282–282.
[28] E.M. Areman, T. Simonis, C. Carter, E.J. Read, and H.G. Klein, *Bulk cryopreservation of lymphocytes in glycerol*, Transfusion 27 (1987), pp. 508–508.
[29] R. Fisher, C.W. Putnam, L.J. Koep, I.G. Sipes, A.J. Gandolfi, and K. Brendel, *Cryopreservation of pig and human liver slices*, Cryobiology 28 (1991), pp. 131–142.
[30] O. Hovatta, *Cryopreservation of testicular tissue in young cancer patients*, Hum. Reprod. Update 7 (2001), pp. 378–383.
[31] D. Kami, M. Uenohata, T. Suzuki, and K. Oosawa, *Cryopreservation of black chokeberry* in vitro *shoot apices*, Cryoletters 29 (2008), pp. 209–216.
[32] A. Farshad and S. Akhondzadeh, *Effects of sucrose and glycerol during the freezing step of cryopreservation on the viability of goat spermatozoa*, Asian-australas. J. Anim. Sci. 21 (2008), pp. 1721–1727.
[33] A. Konstantinow, W. Muhlbauer, A. Hartinger, and G.G.H. Vondonnersmarck, *Skin banking–A simple method for cryopreservation of split-thickness skin and cultured human epidermal-keratinocytes*, Ann. Plast. Surg. 26 (1991), pp. 89–97.
[34] G.M. Hartshorne, K. Elder, J. Crow, H. Dyson, and R.G. Edwards, *The influence of* in vitro *development upon postthaw survival and implantation of cryopreserved human blastocysts*, Hum. Reprod. 6 (1991), pp. 136–141.
[35] H. Abou-Rachid, L.S. Lussier, S. Ringuette, X. Lafleur-Lambert, M. Jaidann, and J. Brisson, *On the correlation between miscibility and solubility properties of energetic plasticizers/polymer blends: Modeling and simulation studies*, Propellants Explosives Pyrotechnics 33 (2008), pp. 301–310.
[36] A. Maitra and S. Bagchi, *Study of solute–solvent and solvent–solvent interactions in pure and mixed binary solvents*, J. Mol. Liq. 137 (2008), pp. 131–137.
[37] S.S. Jawalkar, K.V.S.N. Raju, S.B. Halligudi, M. Sairam, and T.M. Aminabhavi, *Molecular modeling simulations to predict compatibility of poly(vinyl alcohol) and chitosan blends: A comparison with experiments*, J. Phys. Chem. B 111 (2007), pp. 2431–2439.
[38] S.S. Jawalkar and T.M. Aminabhavi, *Molecular modeling simulations and thermodynamic approaches to investigate compatibility/incompatibility of poly(L-lactide) and poly(vinyl alcohol) blends*, Polymer 47 (2006), pp. 8061–8071.
[39] Z.A. Rycerz and P.W.M. Jacobs, *Ewald summation in the molecular-dynamics simulation of large ionic systems–The cohesive energy*, Mol. Simul. 8 (1992), pp. 197–213.
[40] R. Pramanik, P.K. Das, and S. Bagchi, *Solubility and solvation interaction in neat and mixed binary solvents*, Ind. J. Chem. Sect. a-Inorg. Bio-Inorg. Phys. Theor. Anal. Chem. 38 (1999), pp. 906–912.
[41] C.Q. Sun, *Size dependence of nanostructures: Impact of bond order deficiency*, Prog. Solid State Chem. 35 (2007), pp. 1–159.
[42] D.X. Li, B.L. Liu, Y.S. Liu, and C.L. Chen, *Predict the glass transition temperature of glycerol–water binary cryoprotectant by molecular dynamic simulation*, Cryobiology 56 (2008), pp. 114–119.
[43] D. Dantchev, H.W. Diehl, and D. Gruneberg, *Excess free energy and Casimir forces in systems with long-range interactions of van der Waals type: General considerations and exact spherical-model results*, Phys. Rev. E 73 (2006).
[44] T.C. Lim, *On the applicability of mathematical constants and sequences in intermolecular potential energy functions*, J. Math. Chem. 41 (2007), pp. 381–391.
[45] P.P. Ewald, *The calculation of optical and electrostatic grid potential*, Annalen Der Physik 64 (1921), pp. 253–287.
[46] J.Y. Wang, Y.Q. Deng, and B. Roux, *Absolute binding free energy calculations using MD simulations with restraining potentials*, Biophys. J. 91 (2006), pp. 2798–2814.
[47] E. Stefanis, L. Tsivintzelis, and C. Panayiotou, *The partial solubility parameters: An equation-of-state approach*, Fluid Phase Equilibr. 240 (2006), pp. 144–154.
[48] P. Loubeyre, R. LeToullec, E. Wolanin, M. Hanfland, and D. Husermann, *Modulated phases and proton centring in ice observed by X-ray diffraction up to 170 GPa*, Nature 397 (1999), pp. 503–506.
[49] A. Soldera, *Comparison between the glass transition temperatures of the two PMMA tacticities: A molecular dynamics simulation point of view*, Macromol. Symp. 133 (1998), pp. 21–32.